Journal of Systems Engineering and Electronics
Vol. 28, No. 3, June 2017, pp.536 – 545

Missile autopilot design based on robust LPV control

Yuanchuan Shen[1], Jianqiao Yu[1,*], Guanchen Luo[2], and Yuesong Mei[1]

1. School of Aerospace Engineering, Beijing Institute of Technology, Beijing 100081, China;
2. China Academy of Space Technology, Beijing 100086, China

Abstract: This paper proposes an effective algorithm to work out the linear parameter-varying (LPV) framework autopilot for the air defense missile so as to simultaneously guarantee the closed-loop system properties globally and locally, which evidently reduces the number of unknown variables and hence increases the computational efficiency. The notion of "robust quadratic stability" is inducted to meet the global properties, including the robust stability and robust performance, while the regional pole placement scheme together with the adoption of a model matching structure is involved to satisfy the dynamic performance, including limiting the "fast poles". In order to reduce the conservatism, the full block multiplier is employed to depict the properties, with all specifications generalized in integral quadratic constraint frame and finally transformed into linear matrix inequalities for tractable solutions through convex optimization. Simulation results validate the performance of the designed robust LPV autopilot and the proposed framework control method integrating with the full block multiplier approach and the regional pole placement scheme, and demonstrate the efficiency of the algorithm. An efficient algorithm for the air defense missile is proposed to satisfy the required global stability and local dynamical properties by a varying controller according to the flight conditions, and shows sufficient promise in the computational efficiency and the real-time performance of the missile-borne computer system.

Keywords: linear parameter-varying (LPV), full-block multiplier, integral quadratic constraint, regional pole placement, linear matrix inequality.

DOI: 10.21629/JSEE.2017.03.13

1. Introduction

Modern high-performance flight vehicles, including the highly agile missiles and aircraft, operate over a wide range of flight conditions, resulting in substantially varying of dynamic response characteristics during a typical mission [1]. The highly nonlinear dynamics with uncertain, large-scale and rapidly varying parameters are coupled with significant constraints on controller bandwidth, challenging controller the design of autopilots [2]. Consequently, synthesis problems are fain to face the widely time-varying, strongly nonlinear and parameter-dependent dynamic systems instead of traditional linear time invariant (LTI) systems.

Although the classical so-called "gain scheduling" approach has been widely applied, obvious drawbacks may ruin the further application. This approach to developing a varying controller is to design several LTI controllers at a finite number of fixed operating points and connect them with certain blending or interpolation algorithm [2,3]. Due to lack of theoretical guidance, global performance and robustness are not guaranteed, even though the individual local point design may have excellent robustness and performance properties [3,4]. Meanwhile, it is also a time consuming and tedious process [3]. Similar problems might occur in sliding mode control, variable structure control and dynamic inverse control, etc.

Fortunately, with the development of the control theory, in particular robust control theory, a promising linear parameter-varying (LPV) control approach with a firm theoretical basis has emerged since 1990s [5,6]. While the use of parameter-dependent Lyapunov functions [7,8] provides some advantages over the integral quadratic constraint (IQC) frame, they will not extend to very different types of perturbation blocks by the multipliers [9,10]. For the sake of convenience of analysis and synthesis, the dynamic multiplier is adopted to release the constraints of the rate of the varying parameters [11,12]. There are two central ideas behind the multiplier approach: (i) pull the time-varying parameters of the plant out and treat them as one uncertainty block of the uncertainties, and (ii) assume that the controller connects with the time-varying parameters under a linear fractional transformation form. Many well-known results, including system analysis and control synthesis [6,13,14], can be viewed as special cases of the IQC approach.

Despite profound researches on the global performance of the IQC based system, the local properties, especially the dynamic properties, are not evidently demonstrated

Manuscript received October 26, 2015.
*Corresponding author.
This work was supported by the National Natural Science Foundation of China (11532002).

in the IQC frame. However, the basic motivation of gain scheduling techniques, that is, to ensure the local robustness properties, is ineffaceable, which is the fundamental characteristic different from other methodologies such as adaptive control. Particularly for high-performance flight vehicles, in order to satisfy the requirements of the task in the presence of environmental variations, system perturbations and disturbances, the system dynamics and the system gain errors are strictly confined. It is indicated that despite global properties, critical aspects of high-performance flight vehicles handling qualities have to be taken into account, which is mainly concerned with the dynamics of the initial, or transient response to controls.

With attractive peculiarity, the LPV gain scheduling approach draws people's attention immediately in aircraft control field once it is proposed. For example, the approach was utilized to design a robust gain scheduling autopilot with flight altitude and Mach number as scheduling variables for F-18 aircraft [15]. The approach was implemented to design a robust gain scheduling autopilot with dynamic pressure as a scheduling variable for a high-performance aircraft and F-16 VISTA aircraft respectively [1,3]. Then a robust gain scheduling autopilot with flight velocity as scheduling variable for a helicopter unmanned aerial vehicle (UAV) was constructed [16], and the approach was used to design a robust gain scheduling autopilot with the flight altitude, Mach number and angle of attack as scheduling variables for an air defense missile [17]. However, without exception, the multipliers adopted by all of these applications are block-diagonal, and the obtained gain scheduling autopilots show obvious conservatism.

The desired performance properties can be achieved to a certain extent by a model matching structure. The required performance specifications are embodied into a simple reference model, and then the reference command is input to the reference model and the design loop respectively. Finally, the difference between target loop output and design loop output fulfills the requirements indirectly. In many literatures, this scheme is employed [18].

However, this model matching scheme is unable to limit the fast modes of the designed controller [19]. Indeed, for the real control system, especially for high-performance flight vehicles, the existence of fast modes in the controller will put forward high demand for the capability of the vehicle-mounted computer, executive instruments and sampling rate, which will impairs the real time performance of the control system. By performing Gramian-based model state balance reduction analysis, it is indicated that the fast mode is the last one which can be removed. Moreover, the cost of the rising controller dimension is inevitable. In order to achieve practical engineering application, the fast modes of the LPV framework controller must be limited, and the system dimension should be decreased with the best endeavor. As Chilali and Gahinet [20,21] pointed out, fast controller dynamics can be avoided by prohibiting large closed-loop poles in a prescribed region. Compared with the disability of model matching approach, regional pole placement scheme demonstrates fair pertinence to the two problems, particularly the capability to limit fast modes.

Consequently, it is well worth the effort of determining the location of poles in certain regions with the utilization of a reference model for local properties based on IQC frame in the practical engineering application. In addition, the IQC approach is always regarded as a reformulation of the multiplier approach to a large extent [7]. The choice of the multipliers affects the conservatism of the approach directly. On account of practical application, the regional pole placement problem and the effort to reduce conservatism via an appropriate choice of multipliers have to be integrated into a whole consideration. Three main reasons are analyzed. Firstly, the employment of full block multiplier is obligatory for conservatism reduction. Secondly, in order to adopt the multiplier theory, i.e., appropriate multiplier depicting regional stability should be introduced in the whole consideration to exhibit both global properties and local properties. Thirdly, the computational efficiency should be always under consideration.

Yet few present literatures consider this problem, except for [22]. Although an effort has been made to reduce conservatism by introducing the varying rate of parameters, the really employed multiplier is not a full block type as claimed in the paper, which destines to limit the extents of conservatism reduction [22]. In our previous trial of settlement [23], a frame dealing with both global and local properties has been presented, in which the full block multiplier with none additional assumptions is employed to reduce conservatism.

The present work makes contributions mainly to practical engineering application. On account of the implementation of the exact local properties, a model matching structure is employed. And the fast modes of the controller are restrained via the pole assignment scheme. An effective algorithm that avoids complicated construction of starting point and highly reduces the number of variables is proposed in this paper to improve computational efficiency.

2. Model descriptions

The main goal of this section is to present an LPV model of the air defense missile with scheduling variables. And a linear fractional transformation (LFT) of the closed-loop system is constructed to design an autopilot to satisfy performance properties.

Consider the air defense missile model adopted from [18] and illustrate our algorithm in the sequel for the model matching structure in Fig. 1. Air defense missile dynamics are highly dependent on the flight Mach number Ma and the altitude H, which undergo wide variations during operation. The nonlinear dynamics are described in the following state equation:

$$\begin{bmatrix} \dot{a}_y \\ \dot{q} \end{bmatrix} = \begin{bmatrix} Z_a & Z_q \\ M_a & M_q \end{bmatrix} \begin{bmatrix} a_y \\ q \end{bmatrix} + \begin{bmatrix} Z_\delta \\ M_\delta \end{bmatrix} \delta_z \tag{1}$$

where a_y is the normal acceleration, q is the pitch rate and δ_z is the elevator deflection. Dynamic coefficients Z_a, Z_q, Z_δ, M_a, M_q and M_δ are nonlinear functions of Ma and H. For the sake of transforming (1) to LFT model, the dynamic coefficients are expected to be expressed as a polynomial function of Ma and H. The dynamic coefficients have the expressions as follows:

$$Z_a = -0.921 + 8.505 \times 10^{-5} H - 0.374 Ma +$$

$$2.704 \times 10^{-5} MaH,$$

$$Z_q = -939.1 + 0.107H + 1\,038.5Ma - 0.103MaH,$$

$$Z_\delta = 40.688 - 4.447 \times 10^{-3} H -$$

$$107.480Ma + 0.015MaH,$$

$$M_a = -0.267 + 1.354 \times 10^{-4} H - 0.291Ma -$$

$$1.122 \times 10^{-4} MaH + 0.081Ma^2,$$

$$M_q = 0.467 + 2.646 \times 10^{-4} H - 3.908Ma +$$

$$0.479Ma^2 + 2.751 \times 10^{-5} Ma^2 H,$$

$$M_\delta = 193.240 - 0.028H + 104.781Ma -$$

$$3.528 \times 10^{-3} MaH.$$

By linearly interconnecting all these components depicted in Fig. 1, an equivalent structure is obtained as shown in Fig. 2. $\boldsymbol{G}_a$, $\boldsymbol{G}_r$, $\boldsymbol{W}_p$ denote respectively the actuator dynamics, the reference model and the weighting function, and the expressions are presented in detail in Section 4. a_{yc} is the normal acceleration command, and e_p and a_{yr} are the outputs of $\boldsymbol{W}_p$ and $\boldsymbol{G}_r$.

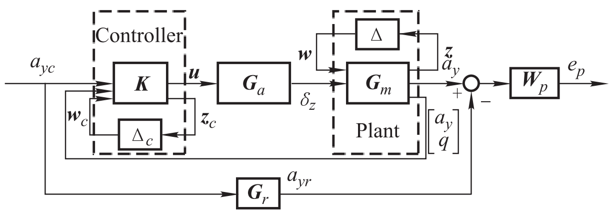

Fig. 1 Model matching structure of the autopilot

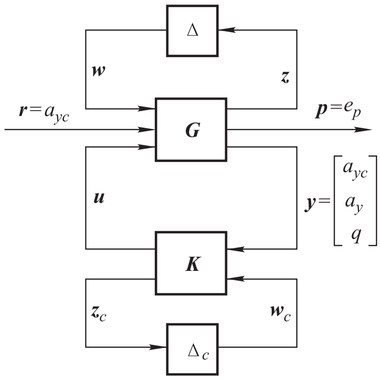

Fig. 2 Equivalent design structure of the autopilot

Consider the plant and controller described by (2) and (3) with the scheduling block Δ and Δ_c in Fig. 2, which are both LFTs composed of the LTI part and the uncertain part.

$$\begin{bmatrix} \dot{\boldsymbol{x}}(t) \\ \boldsymbol{z}(t) \\ \boldsymbol{p}(t) \\ \boldsymbol{y}(t) \end{bmatrix} = \left[\begin{array}{c|ccc} \boldsymbol{A} & \boldsymbol{B}_w & \boldsymbol{B}_r & \boldsymbol{B} \\ \hline \boldsymbol{C}_z & \boldsymbol{D}_{zw} & \boldsymbol{D}_{zr} & \boldsymbol{D}_z \\ \boldsymbol{C}_p & \boldsymbol{D}_{pw} & \boldsymbol{D}_{pr} & \boldsymbol{D}_p \\ \boldsymbol{C} & \boldsymbol{D}_w & \boldsymbol{D}_r & \boldsymbol{O} \end{array}\right] \begin{bmatrix} \boldsymbol{x}(t) \\ \boldsymbol{w}(t) \\ \boldsymbol{r}(t) \\ \boldsymbol{u}(t) \end{bmatrix} \tag{2}$$

$$\boldsymbol{w} = \Delta \boldsymbol{z}$$

$$\begin{bmatrix} \dot{\boldsymbol{x}}_c(t) \\ \boldsymbol{u}(t) \\ \boldsymbol{z}_c(t) \end{bmatrix} = \left[\begin{array}{c|cc} \boldsymbol{A}_c & \boldsymbol{B}_{c1} & \boldsymbol{B}_{c2} \\ \hline \boldsymbol{C}_{c1} & \boldsymbol{D}_{c11} & \boldsymbol{D}_{c12} \\ \boldsymbol{C}_{c2} & \boldsymbol{D}_{c21} & \boldsymbol{D}_{c22} \end{array}\right] \begin{bmatrix} \boldsymbol{x}_c(t) \\ \boldsymbol{y}(t) \\ \boldsymbol{w}_c(t) \end{bmatrix} \tag{3}$$

$$\boldsymbol{w}_c = \Delta_c \boldsymbol{z}_c$$

where the time-varying parameters Ma and H are lumped into the uncertain block Δ. The $\mathrm{col}(\boldsymbol{x}, \boldsymbol{w}, \boldsymbol{r}, \boldsymbol{u}) \in \mathbf{R}^{n \times m \times n_r \times n_u}$ and $\mathrm{col}(\boldsymbol{z}, \boldsymbol{p}, \boldsymbol{y}) \in \mathbf{R}^{k \times n_p \times n_y}$ respectively denote the collection of state, exogenous input, reference command, control input and output corresponding to "uncertainties", output in performance channel and measurement output channel. Similar denotation is for (3) with the subscript "c" standing for the controller.

Then, the closed-loop system is denoted as (4) with $\boldsymbol{x}_{cl} = [\boldsymbol{x}^{\mathrm{T}}, \boldsymbol{x}_c^{\mathrm{T}}]^{\mathrm{T}}$, $\boldsymbol{z}_{cl} = [\boldsymbol{z}^{\mathrm{T}}, \boldsymbol{z}_c^{\mathrm{T}}]^{\mathrm{T}}$, $\boldsymbol{w}_{cl} = [\boldsymbol{w}^{\mathrm{T}}, \boldsymbol{w}_c^{\mathrm{T}}]^{\mathrm{T}}$ and $\Delta_{cl} = \mathrm{diag}(\Delta,\ \Delta_c)$.

$$\begin{bmatrix} \dot{\boldsymbol{x}}_{cl} \\ \boldsymbol{z}_{cl} \\ \boldsymbol{p} \end{bmatrix} = \left[\begin{array}{c|cc} \boldsymbol{A}_{cl} & \boldsymbol{B}_{cl} & \boldsymbol{B}_{cl} \\ \hline \boldsymbol{C}_{cl} & \boldsymbol{D}_{cl} & \boldsymbol{D}_{clr} \\ \boldsymbol{C}_{clp} & \boldsymbol{D}_{clp} & \boldsymbol{D}_{clpr} \end{array}\right] \begin{bmatrix} \boldsymbol{x}_{cl} \\ \boldsymbol{w}_{cl} \\ \boldsymbol{r} \end{bmatrix} \tag{4}$$

$$\boldsymbol{w}_{cl} = \Delta_{cl} \boldsymbol{z}_{cl}.$$

Thus, the autopilot design problem is converted into the synthesis of an LPV controller that dynamically processes the measurement output $\boldsymbol{y}$ and scheduling variables to ensure control input $\boldsymbol{u}$ that robustly stabilizes the interconnection system in Fig. 2, and renders the $\mathcal{H}_\infty$-gain from $\boldsymbol{r}$ to $\boldsymbol{p}$ less than $\gamma > 0$ while the poles of the controller are restricted in the logical region to avoid the "fast modes".

3. Efficient algorithm

The global properties can be described in robust quadratic performance and local properties in regional stability.

Lemma 1 [24] Robust quadratic performance is achieved for (4) if there exist $\boldsymbol{X} > 0$ and a symmetric multiplier $\boldsymbol{R} = \begin{bmatrix} \boldsymbol{P} & \boldsymbol{S} \\ \boldsymbol{S}^{\mathrm{T}} & \boldsymbol{Q} \end{bmatrix}$ such that (5), (6) hold true:

$$(\bullet)^{\mathrm{T}} \boldsymbol{R} \begin{bmatrix} \Delta_{cl} \\ \boldsymbol{I} \end{bmatrix} > 0, \quad \forall \Delta_{cl} \tag{5}$$

$$(\bullet)^{\mathrm{T}} \left[\begin{array}{cc|c|c} \boldsymbol{O} & \boldsymbol{X} & & \\ \boldsymbol{X} & \boldsymbol{O} & & \\ \hline & & \boldsymbol{R} & \\ \hline & & & \boldsymbol{R}_p \end{array}\right] \left[\begin{array}{ccc} \boldsymbol{I} & \boldsymbol{O} & \boldsymbol{O} \\ \boldsymbol{A}_{cl} & \boldsymbol{B}_{cl} & \boldsymbol{B}_{clr} \\ \hline \boldsymbol{O} & \boldsymbol{I} & B \\ \boldsymbol{C}_{cl} & \boldsymbol{D}_{cl} & \boldsymbol{D}_{clr} \\ \hline \boldsymbol{O} & \boldsymbol{O} & \boldsymbol{I} \\ \boldsymbol{C}_{clp} & \boldsymbol{D}_{clp} & \boldsymbol{D}_{clpr} \end{array}\right] < 0. \tag{6}$$

Lemma 2 [20] Robust D-stability is achieved for (4) if there exist $\boldsymbol{X}_D > 0$ and a symmetric multiplier $\mathbf{R}_D = \begin{bmatrix} \boldsymbol{P}_D & \boldsymbol{S}_D \\ \boldsymbol{S}_D^{\mathrm{T}} & \boldsymbol{Q}_D \end{bmatrix}$ such that (7), (8) hold true:

$$(\bullet)^{\mathrm{T}} \boldsymbol{R}_D \begin{bmatrix} \Delta_{cl} \\ \boldsymbol{I} \end{bmatrix} > 0, \quad \forall \Delta_{cl} \tag{7}$$

$$\begin{bmatrix} \mathcal{M}_D(\boldsymbol{A}_{cl}, \boldsymbol{X}_D) & \boldsymbol{M} \otimes \boldsymbol{X}_D \boldsymbol{B}_{cl} & \boldsymbol{I} \otimes \boldsymbol{C}_{cl}^{\mathrm{T}} \\ \boldsymbol{M}^{\mathrm{T}} \otimes (\boldsymbol{X}_D \boldsymbol{B}_{cl})^{\mathrm{T}} & \boldsymbol{I} \otimes (\boldsymbol{P}_D - \boldsymbol{S}_D \boldsymbol{Q}_D^{-1} \boldsymbol{S}_D^{\mathrm{T}}) & \boldsymbol{I} \otimes (\boldsymbol{D}_{cl}^{\mathrm{T}} + \boldsymbol{S}_D \boldsymbol{Q}_D^{-1}) \\ \boldsymbol{I} \otimes \boldsymbol{C}_{cl} & \boldsymbol{I} \otimes (\boldsymbol{D}_{cl} + \boldsymbol{Q}_D^{-1} \boldsymbol{S}_D^{\mathrm{T}}) & -\boldsymbol{I} \otimes \boldsymbol{Q}_D^{-1} \end{bmatrix} < 0 \tag{8}$$

where

$$\mathcal{M}_D(\boldsymbol{A}_{cl}, \boldsymbol{X}_D) :=$$
$$\boldsymbol{L} \otimes \boldsymbol{X} + \boldsymbol{M} \otimes (\boldsymbol{X}_D \boldsymbol{A}_{cl}) + \boldsymbol{M}^{\mathrm{T}} \otimes (\boldsymbol{X}_D \boldsymbol{A}_{cl})^{\mathrm{T}}.$$

In Lemma 1 and Lemma 2, multipliers $\boldsymbol{R}_p = \begin{bmatrix} \boldsymbol{P}_p & \boldsymbol{S}_p \\ \boldsymbol{S}_p^{\mathrm{T}} & \boldsymbol{Q}_p \end{bmatrix}$, $\boldsymbol{L}$ and $\boldsymbol{M}$ denote performance properties, and their forms can be referred to [20] and [24]. Our goal is to enforce the robust quadratic performance with the poles constrained in arbitrary linear matrix inequality (LMI) regions. Directly combining Lemma 1 with Lemma 2, the robust quadratic performance and the regional stability are guaranteed.

An accessible settlement is to decompose the solving process into two stages. The first action is to calculate appropriate $\boldsymbol{R}$ and $\boldsymbol{R}_D$. Secondly, given the worked-out $\boldsymbol{R}$ and $\boldsymbol{R}_D$ as known variables to solve the controller $\boldsymbol{K}$, Δ_c, and Lyapunov matrices $\boldsymbol{X}$ and $\boldsymbol{X}_D$ via (5), (6), (7) and (8). Based on that thought, we have the following algorithm.

Step 1 Judge whether there exist controller(s) such that robust quadratic performance and performance properties could be achieved.

Enforcing the convexity by seeking a common Lyapunov matrix $\boldsymbol{X} = \boldsymbol{X}_D > 0$ and a common multiplier $\boldsymbol{R} = \boldsymbol{R}_D$, we have the following theorem.

Theorem 1 The robust quadratic performance is achieved for the closed-loop LPV system (3) with the regional pole constraints satisfied if there exist $\boldsymbol{U}_1, \boldsymbol{U}_2$, $\boldsymbol{V}_1 > 0$, $\boldsymbol{V}_2 < 0$, $\boldsymbol{W}_1$, $\boldsymbol{W}_2, \boldsymbol{T}_1, \boldsymbol{T}_2$, and a couple of symmetric matrices $\overline{\boldsymbol{X}}_D$ and $\overline{\boldsymbol{Y}}_D$ such that (9) – (19) hold true:

$$(\bullet)^{\mathrm{T}} \left[\begin{array}{cc|cc|c} \boldsymbol{O} & \overline{\boldsymbol{X}}_D & & & \\ \overline{\boldsymbol{X}}_D & \boldsymbol{O} & & & \\ \hline & & \boldsymbol{V}_2 & \boldsymbol{W}_2 & \\ & & \boldsymbol{W}_2^{\mathrm{T}} & \boldsymbol{U}_2 & \\ \hline & & & & \boldsymbol{R}_p \end{array}\right] \cdot \left(\left[\begin{array}{ccc} \boldsymbol{I} & \boldsymbol{O} & \boldsymbol{O} \\ \boldsymbol{A} & \boldsymbol{B}_w & \boldsymbol{B}_r \\ \hline \boldsymbol{O} & \boldsymbol{I} & \boldsymbol{O} \\ \boldsymbol{C}_z & \boldsymbol{D}_{zw} & \boldsymbol{D}_{zr} \\ \hline \boldsymbol{O} & \boldsymbol{O} & \boldsymbol{I} \\ \boldsymbol{C}_p & \boldsymbol{D}_{pw} & \boldsymbol{D}_{pr} \end{array}\right] \begin{bmatrix} \ker \boldsymbol{C} \\ \ker \boldsymbol{D}_w \\ \ker \boldsymbol{D}_r \end{bmatrix} \right) < 0 \tag{9}$$

$$(\bullet)^{\mathrm{T}} \left[\begin{array}{cc|cc|c} \boldsymbol{O} & \overline{\boldsymbol{Y}}_D & & & \\ \overline{\boldsymbol{Y}}_D & \boldsymbol{O} & & & \\ \hline & & \boldsymbol{U}_1 & \boldsymbol{W}_1 & \\ & & \boldsymbol{W}_1^{\mathrm{T}} & \boldsymbol{V}_1 & \\ \hline & & & & \boldsymbol{R}_p^{-1} \end{array}\right] \cdot \left(\left[\begin{array}{ccc} -\boldsymbol{A}^{\mathrm{T}} & -\boldsymbol{C}_z^{\mathrm{T}} & -\boldsymbol{C}_p^{\mathrm{T}} \\ \boldsymbol{I} & \boldsymbol{O} & \boldsymbol{B} \\ \hline -\boldsymbol{B}_w^{\mathrm{T}} & -\boldsymbol{D}_{zw}^{\mathrm{T}} & -\boldsymbol{D}_{pw}^{\mathrm{T}} \\ \boldsymbol{O} & \boldsymbol{I} & \boldsymbol{O} \\ \hline -\boldsymbol{B}_r^{\mathrm{T}} & -\boldsymbol{D}_{zr}^{\mathrm{T}} & -\boldsymbol{D}_{pr}^{\mathrm{T}} \\ \boldsymbol{O} & \boldsymbol{O} & \boldsymbol{I} \end{array}\right] \begin{bmatrix} \ker \boldsymbol{B}^{\mathrm{T}} \\ \ker \boldsymbol{D}_z^{\mathrm{T}} \\ \ker \boldsymbol{D}_p^{\mathrm{T}} \end{bmatrix} \right) < 0 \tag{10}$$

$$(\bullet)^{\mathrm{T}} \begin{bmatrix} \boldsymbol{\psi}_1 & \boldsymbol{\psi}_{12} \\ \boldsymbol{\psi}_{12}^{\mathrm{T}} & \boldsymbol{\psi}_2 \end{bmatrix} \begin{bmatrix} \boldsymbol{I} \otimes \ker \boldsymbol{B}^{\mathrm{T}} & \boldsymbol{O} \\ \boldsymbol{O} & \boldsymbol{I} \otimes \ker \boldsymbol{D}_z^{\mathrm{T}} \end{bmatrix} < 0 \tag{11}$$

$$(\bullet)^{\mathrm{T}} \begin{bmatrix} \boldsymbol{\varphi}_1 & \boldsymbol{\varphi}_{12} \\ \boldsymbol{\varphi}_{12}^{\mathrm{T}} & \boldsymbol{\varphi}_2 \end{bmatrix} \begin{bmatrix} \boldsymbol{I} \otimes \ker \boldsymbol{C} & \boldsymbol{O} \\ \boldsymbol{O} & \boldsymbol{I} \otimes \ker \boldsymbol{D}_w \end{bmatrix} < 0 \tag{12}$$

$$\Delta^{\mathrm{T}} \boldsymbol{V}_2 \Delta + \Delta^{\mathrm{T}} \boldsymbol{W}_2 + \boldsymbol{W}_2^{\mathrm{T}} \Delta + \boldsymbol{U}_2 > 0 \tag{13}$$

$$\Delta \boldsymbol{V}_1 \Delta^{\mathrm{T}} + \Delta \boldsymbol{W}_1^{\mathrm{T}} + \boldsymbol{W}_1 \Delta^{\mathrm{T}} + \boldsymbol{U}_1 < 0 \tag{14}$$

$$\begin{bmatrix} \overline{\boldsymbol{X}}_D & \boldsymbol{I} \\ \boldsymbol{I} & \overline{\boldsymbol{Y}}_D \end{bmatrix} \geqslant 0 \tag{15}$$

$$\begin{bmatrix} \boldsymbol{V}_1 - \boldsymbol{T}_2 & \boldsymbol{I} \\ \boldsymbol{I} & \boldsymbol{U}_2 \end{bmatrix} \geqslant 0 \tag{16}$$

$$\begin{bmatrix} \boldsymbol{V}_2 - \boldsymbol{T}_1 & \boldsymbol{I} \\ \boldsymbol{I} & \boldsymbol{U}_1 \end{bmatrix} \leqslant 0 \tag{17}$$

$$\begin{bmatrix} \boldsymbol{T}_1 & \boldsymbol{W}_2 \\ \boldsymbol{W}_2^{\mathrm{T}} & \boldsymbol{U}_2 \end{bmatrix} \geqslant 0 \tag{18}$$

$$\begin{bmatrix} \boldsymbol{U}_1 & \boldsymbol{W}_1 \\ \boldsymbol{W}_1^{\mathrm{T}} & \boldsymbol{T}_2 \end{bmatrix} \leqslant 0 \tag{19}$$

where

$$\overline{\mathcal{M}}_D(\boldsymbol{A}, \overline{\boldsymbol{Y}}_D) = \boldsymbol{L} \otimes \overline{\boldsymbol{Y}}_D + \boldsymbol{M} \otimes (\boldsymbol{A}\overline{\boldsymbol{Y}}_D) + \boldsymbol{M}^{\mathrm{T}} \otimes (\boldsymbol{A}\overline{\boldsymbol{Y}}_D)^{\mathrm{T}},$$

$$\boldsymbol{\psi}_1 = \overline{\mathcal{M}}_D(\boldsymbol{A}, \overline{\boldsymbol{Y}}_D) - (\boldsymbol{M}\boldsymbol{M}^{\mathrm{T}}) \otimes (\boldsymbol{B}_w \boldsymbol{U}_1 \boldsymbol{B}_w^{\mathrm{T}}),$$

$$\boldsymbol{\psi}_{12} = \boldsymbol{I} \otimes \overline{\boldsymbol{Y}}_D^{\mathrm{T}} \boldsymbol{C}_z^{\mathrm{T}} - \boldsymbol{M} \otimes \boldsymbol{B}_w (\boldsymbol{U}_1 \boldsymbol{D}_{zw}^{\mathrm{T}} + \boldsymbol{W}_1),$$

$$\boldsymbol{\psi}_2 = -\boldsymbol{I} \otimes (\boldsymbol{V}_1 + \boldsymbol{D}_{zw} \boldsymbol{U}_1 \boldsymbol{D}_{zw}^{\mathrm{T}} + \boldsymbol{W}_1^{\mathrm{T}} \boldsymbol{D}_{zw}^{\mathrm{T}} + \boldsymbol{D}_{zw} \boldsymbol{W}_1),$$

$$\boldsymbol{\varphi}_1 = \overline{\mathcal{M}}_D(\boldsymbol{A}, \overline{\boldsymbol{X}}_D) + \boldsymbol{I} \otimes (\boldsymbol{C}_z^{\mathrm{T}} \boldsymbol{U}_2 \boldsymbol{C}_z),$$

$$\boldsymbol{\varphi}_{12} = \boldsymbol{M} \otimes \overline{\boldsymbol{X}}_D \boldsymbol{B}_w + \boldsymbol{I} \otimes \boldsymbol{C}_z^{\mathrm{T}} (\boldsymbol{U}_2 \boldsymbol{D}_{zw} + \boldsymbol{W}_2^{\mathrm{T}}),$$

$$\boldsymbol{\varphi}_2 = \boldsymbol{I} \otimes (\boldsymbol{V}_2 + \boldsymbol{W}_2 \boldsymbol{D}_{zw} + \boldsymbol{D}_{zw}^{\mathrm{T}} \boldsymbol{W}_2^{\mathrm{T}} + \boldsymbol{D}_{zw}^{\mathrm{T}} \boldsymbol{U}_2 \boldsymbol{D}_{zw}).$$

Proof See references [23–25] and the references therein. □

Indeed, the assumption $\boldsymbol{X} = \boldsymbol{X}_D$, $\boldsymbol{R} = \boldsymbol{R}_D$ is a compromise between computational efficiency and conservatism. If it is removed, no conservatism will be introduced into the theorem. On the other hand, to distinguish among $\boldsymbol{X}$, $\boldsymbol{R}$ and $\boldsymbol{X}_D, \boldsymbol{R}_D$ will introduce more unknown variables, which in consequence highly increases the difficulty in solving the problem.

Step 2 Work out an $\boldsymbol{R}$ (or $\boldsymbol{R}_D$ as well) such that (5) holds.

Denote

$$\boldsymbol{R}_1 = \begin{bmatrix} \boldsymbol{V}_2 & \boldsymbol{W}_2 \\ \boldsymbol{W}_2^{\mathrm{T}} & \boldsymbol{U}_2 \end{bmatrix}, \quad \widetilde{\boldsymbol{R}}_1 = \begin{bmatrix} \boldsymbol{U}_1 & -\boldsymbol{W}_1 \\ -\boldsymbol{W}_1^{\mathrm{T}} & \boldsymbol{V}_1 \end{bmatrix}.$$

With eigenvalue decomposition, $\boldsymbol{R}_1 - \widetilde{\boldsymbol{R}}_1^{-1}$ can be decomposed as

$$\boldsymbol{R}_1 - \widetilde{\boldsymbol{R}}_1^{-1} = \boldsymbol{\Gamma} \begin{bmatrix} -\boldsymbol{\Sigma}_- & \boldsymbol{O} \\ \boldsymbol{O} & \boldsymbol{\Sigma}_+ \end{bmatrix} \boldsymbol{\Gamma}^{\mathrm{T}} \tag{20}$$

where $\boldsymbol{\Sigma}_-, \boldsymbol{\Sigma}_+ > 0$. Then, for an arbitrary and invertible $\boldsymbol{U}$, the full block multiplier $\boldsymbol{R}$ can be reconstructed by

$$\boldsymbol{R} = (\bullet)^{\mathrm{T}} \begin{bmatrix} \boldsymbol{R}_1 & \boldsymbol{R}_{12} \\ \boldsymbol{R}_{12}^{\mathrm{T}} & \boldsymbol{R}_2 \end{bmatrix} \left(\begin{bmatrix} \boldsymbol{I} & \boldsymbol{O} \\ \boldsymbol{O} & \boldsymbol{U} \end{bmatrix} \boldsymbol{I}_e \right) \tag{21}$$

$$\boldsymbol{R}_{12} = \boldsymbol{\Gamma} \begin{bmatrix} \boldsymbol{\Sigma}_-^{1/2} & \boldsymbol{O} \\ \boldsymbol{O} & \boldsymbol{\Sigma}_+^{1/2} \end{bmatrix}, \quad \boldsymbol{R}_2 = \begin{bmatrix} -\boldsymbol{I} & \boldsymbol{O} \\ \boldsymbol{O} & \boldsymbol{I} \end{bmatrix}$$

$$\boldsymbol{I}_e = \left[\begin{array}{cc|cc} \boldsymbol{I} & \boldsymbol{O} & \boldsymbol{O} & \boldsymbol{O} \\ \boldsymbol{O} & \boldsymbol{O} & \boldsymbol{I} & \boldsymbol{O} \\ \hline \boldsymbol{O} & \boldsymbol{I} & \boldsymbol{O} & \boldsymbol{O} \\ \boldsymbol{O} & \boldsymbol{O} & \boldsymbol{O} & \boldsymbol{I} \end{array}\right].$$

Step 3 For that specified $\boldsymbol{R}$, $\boldsymbol{K}$ and Δ_c can be calculated such that (5), (6) and (8) hold.

$\boldsymbol{R}$ can be parted as $\begin{bmatrix} \boldsymbol{P} & \boldsymbol{S} \\ \boldsymbol{S}^{\mathrm{T}} & \boldsymbol{Q} \end{bmatrix}$, and denote $\widehat{\boldsymbol{P}} = \mathrm{blockdiag}\{\boldsymbol{O}, \boldsymbol{P}, \boldsymbol{P}_p\}$, $\widehat{\boldsymbol{S}} = \mathrm{blockdiag}\{\boldsymbol{X}, \boldsymbol{S}, \boldsymbol{S}_p\}$, $\overline{\boldsymbol{Q}} = \mathrm{blockdiag}\{\boldsymbol{Q}, \boldsymbol{Q}_p\}$,

$$\boldsymbol{E}_0 = \begin{bmatrix} \boldsymbol{O} & \boldsymbol{B} & \boldsymbol{O} \\ \boldsymbol{I}_{n_c} & \boldsymbol{O} & \boldsymbol{O} \\ \boldsymbol{O} & \boldsymbol{D}_z & \boldsymbol{O} \\ \boldsymbol{O} & \boldsymbol{O} & \boldsymbol{I}_{k_c} \\ \boldsymbol{O} & \boldsymbol{D}_p & \boldsymbol{O} \end{bmatrix}$$

$$\boldsymbol{F}_0 = \begin{bmatrix} \boldsymbol{O} & \boldsymbol{I}_{n_c} & \boldsymbol{O} & \boldsymbol{O} & \boldsymbol{O} \\ \boldsymbol{C} & \boldsymbol{O} & \boldsymbol{D}_w & \boldsymbol{O} & \boldsymbol{D}_r \\ \boldsymbol{O} & \boldsymbol{O} & \boldsymbol{O} & \boldsymbol{I}_{m_c} & \boldsymbol{O} \end{bmatrix}$$

$$\mathcal{G}_0 = \underbrace{\left[\begin{array}{cc|ccc} \boldsymbol{A} & \boldsymbol{O} & \boldsymbol{B}_w & \boldsymbol{O} & \boldsymbol{B}_r \\ \boldsymbol{O} & \boldsymbol{O}_{n_c} & \boldsymbol{O} & \boldsymbol{O} & \boldsymbol{O} \\ \boldsymbol{C}_z & \boldsymbol{O} & \boldsymbol{D}_{zw} & \boldsymbol{O} & \boldsymbol{D}_{zr} \\ \boldsymbol{O} & \boldsymbol{O} & \boldsymbol{O} & \boldsymbol{O}_{k_c \times m_c} & \boldsymbol{O} \\ \boldsymbol{C}_p & \boldsymbol{O} & \boldsymbol{D}_{pw} & \boldsymbol{O} & \boldsymbol{D}_{pr} \end{array}\right]}_{\boldsymbol{G}_0}.$$

Then we have the following theorem for controller synthesis.

Theorem 2 There exist controller(s) such that original the robust quadratic performance with regional pole placement constraints problem is feasible if there exist $\boldsymbol{X}_1 > 0$, $\boldsymbol{Y}_1 > 0$, and matrices $\boldsymbol{A}_K$, $\boldsymbol{B}_{K1}$, $\boldsymbol{B}_{K2}$, $\boldsymbol{C}_{K1}$, $\boldsymbol{C}_{K2}$, $\boldsymbol{D}_{c11}$, $\boldsymbol{D}_{c12}$, $\boldsymbol{D}_{c21}$, $\boldsymbol{D}_{c22}$ such that (22)–(25) hold true:

$$\begin{bmatrix} \boldsymbol{H}_a + \boldsymbol{H}_a^{\mathrm{T}} & \boldsymbol{H}_b & \boldsymbol{H}_{br} & \boldsymbol{H}_c^{\mathrm{T}} & \boldsymbol{H}_{cp}^{\mathrm{T}} \\ \boldsymbol{H}_b^{\mathrm{T}} & \boldsymbol{P} & \boldsymbol{O} & \boldsymbol{H}_d^{\mathrm{T}} + \boldsymbol{S}\boldsymbol{Q}^{-1} & \boldsymbol{H}_{dp}^{\mathrm{T}} \\ \boldsymbol{H}_{br}^{\mathrm{T}} & \boldsymbol{O} & \boldsymbol{P}_p & \boldsymbol{H}_{dr}^{\mathrm{T}} & \boldsymbol{H}_{dpr}^{\mathrm{T}} + \boldsymbol{S}_p \boldsymbol{Q}_p^{-1} \\ \boldsymbol{H}_c & \boldsymbol{H}_d + \boldsymbol{Q}^{-1}\boldsymbol{S}^{\mathrm{T}} & \boldsymbol{H}_{dr} & -\boldsymbol{Q}^{-1} & \boldsymbol{O} \\ \boldsymbol{H}_{cp} & \boldsymbol{H}_{dp} & \boldsymbol{H}_{dpr} + \boldsymbol{Q}_p^{-1}\boldsymbol{S}_p^{\mathrm{T}} & \boldsymbol{O} & -\boldsymbol{Q}_p^{-1} \end{bmatrix} < 0 \tag{22}$$

$$\begin{bmatrix} \boldsymbol{L} \otimes \begin{bmatrix} \boldsymbol{X}_1 & \boldsymbol{I} \\ \boldsymbol{I} & \boldsymbol{Y}_1 \end{bmatrix} + \boldsymbol{M} \otimes \boldsymbol{H}_a + \boldsymbol{M}^{\mathrm{T}} \otimes \boldsymbol{H}_a^{\mathrm{T}} < 0 & \boldsymbol{M} \otimes \boldsymbol{H}_b & \boldsymbol{I} \otimes \boldsymbol{H}_c^{\mathrm{T}} \\ \boldsymbol{M}^{\mathrm{T}} \otimes \boldsymbol{H}_b^{\mathrm{T}} & \boldsymbol{I} \otimes (\boldsymbol{P} - \boldsymbol{S}\boldsymbol{Q}^{-1}\boldsymbol{S}^{\mathrm{T}}) & \boldsymbol{I} \otimes (\boldsymbol{H}_d^{\mathrm{T}} + \boldsymbol{S}\boldsymbol{Q}^{-1}) \\ \boldsymbol{I} \otimes \boldsymbol{H}_c & \boldsymbol{I} \otimes (\boldsymbol{H}_d + \boldsymbol{Q}^{-1}\boldsymbol{S}^{\mathrm{T}}) & -\boldsymbol{I} \otimes \boldsymbol{Q}^{-1} \end{bmatrix} < 0 \tag{23}$$

$$\begin{bmatrix} \boldsymbol{X}_1 & \boldsymbol{I} \\ \boldsymbol{I} & \boldsymbol{Y}_1 \end{bmatrix} > 0 \tag{24}$$

$$\begin{bmatrix} \widehat{\boldsymbol{P}} + \widehat{\boldsymbol{S}}(\boldsymbol{G}_0 + \boldsymbol{E}_0\boldsymbol{K}\boldsymbol{F}_0) + (\boldsymbol{G}_0 + \boldsymbol{E}_0\boldsymbol{K}\boldsymbol{F}_0)^{\mathrm{T}}\widehat{\boldsymbol{S}}^{\mathrm{T}} & (\boldsymbol{G}_0 + \boldsymbol{E}_0\boldsymbol{K}\boldsymbol{F}_0)^{\mathrm{T}}\begin{bmatrix} \boldsymbol{O} \\ \boldsymbol{I} \end{bmatrix} \\ \begin{bmatrix} \boldsymbol{O} & \boldsymbol{I} \end{bmatrix}(\boldsymbol{G}_0 + \boldsymbol{E}_0\boldsymbol{K}\boldsymbol{F}_0) & -\overline{\boldsymbol{Q}}^{-1} \end{bmatrix} < 0 \tag{25}$$

with the shorthand notation

$$\boldsymbol{H}_a = \begin{bmatrix} \boldsymbol{X}_1\boldsymbol{A} + \boldsymbol{B}_{K1}\boldsymbol{C} & \boldsymbol{A}_K \\ \boldsymbol{A} + \boldsymbol{B}\boldsymbol{D}_{c11}\boldsymbol{C} & \boldsymbol{A}\boldsymbol{Y}_1^{\mathrm{T}} + \boldsymbol{B}\boldsymbol{C}_{K1} \end{bmatrix}$$

$$\boldsymbol{H}_b = \begin{bmatrix} \boldsymbol{X}_1\boldsymbol{B}_w + \boldsymbol{B}_{K1}\boldsymbol{D}_w & \boldsymbol{B}_{K2} \\ \boldsymbol{B}_w + \boldsymbol{B}\boldsymbol{D}_{c11}\boldsymbol{D}_w & \boldsymbol{B}\boldsymbol{D}_{c12} \end{bmatrix}$$

$$\boldsymbol{H}_{br} = \begin{bmatrix} \boldsymbol{X}_1\boldsymbol{B}_r + \boldsymbol{B}_{K1}\boldsymbol{D}_r \\ \boldsymbol{B}_r + \boldsymbol{B}\boldsymbol{D}_{c11}\boldsymbol{D}_r \end{bmatrix}$$

$$\boldsymbol{H}_c = \begin{bmatrix} \boldsymbol{C}_z + \boldsymbol{D}_z\boldsymbol{D}_{c11}\boldsymbol{C} & \boldsymbol{C}_z\boldsymbol{Y}_1^{\mathrm{T}} + \boldsymbol{D}_z\boldsymbol{C}_{K1} \\ \boldsymbol{D}_{c21}\boldsymbol{C} & \boldsymbol{C}_{K2} \end{bmatrix}$$

$$\boldsymbol{H}_{cp} = \begin{bmatrix} \boldsymbol{C}_p + \boldsymbol{D}_p\boldsymbol{D}_{c11}\boldsymbol{C} & \boldsymbol{C}_p\boldsymbol{Y}_1^{\mathrm{T}} + \boldsymbol{D}_p\boldsymbol{C}_{K1} \end{bmatrix}$$

$$\boldsymbol{H}_d = \begin{bmatrix} \boldsymbol{D}_{zw} + \boldsymbol{D}_z\boldsymbol{D}_{c11}\boldsymbol{D}_w & \boldsymbol{D}_z\boldsymbol{D}_{c12} \\ \boldsymbol{D}_{c12}\boldsymbol{D}_w & \boldsymbol{D}_{c22} \end{bmatrix}$$

$$\boldsymbol{H}_{dp} = \begin{bmatrix} \boldsymbol{D}_{pw} + \boldsymbol{D}_p\boldsymbol{D}_{c11}\boldsymbol{D}_w & \boldsymbol{D}_p\boldsymbol{D}_{c12} \end{bmatrix}$$

$$\boldsymbol{H}_{dr} = \begin{bmatrix} \boldsymbol{D}_{zr} + \boldsymbol{D}_z\boldsymbol{D}_{c11}\boldsymbol{D}_r \\ \boldsymbol{D}_{c21}\boldsymbol{D}_r \end{bmatrix}$$

$$\boldsymbol{H}_{dpr} = \boldsymbol{D}_{pr} + \boldsymbol{D}_p\boldsymbol{D}_{c11}\boldsymbol{D}_r.$$

Proof Transforming the quadratic inequalities (6) and (5) into linear/bilinear form, we have

$$\begin{bmatrix} \boldsymbol{Q} + \Delta_{cl}^{\mathrm{T}}\boldsymbol{S} + \boldsymbol{S}^{\mathrm{T}}\Delta_{cl} & \Delta_{cl}^{\mathrm{T}} \\ \Delta_{cl} & -\boldsymbol{P}^{-1} \end{bmatrix} > 0. \tag{26}$$

Then, (8), (25), and (26) are all linear/bilinear. At the same time, appropriate variable replacement will rewrite the bilinear inequalities into linear form. Define the new controller variables as

$$\boldsymbol{B}_{K1} = \boldsymbol{X}_1\boldsymbol{B}\boldsymbol{D}_{c11} + \boldsymbol{X}_2\boldsymbol{B}_{c1}$$

$$\boldsymbol{B}_{K2} = \boldsymbol{X}_1\boldsymbol{B}\boldsymbol{D}_{c12} + \boldsymbol{X}_2\boldsymbol{B}_{c2}$$

$$\boldsymbol{C}_{K1} = \boldsymbol{D}_{c11}\boldsymbol{C}\boldsymbol{Y}_1^{\mathrm{T}} + \boldsymbol{C}_{c1}\boldsymbol{Y}_2^{\mathrm{T}}$$

$$\boldsymbol{C}_{K2} = \boldsymbol{D}_{c21}\boldsymbol{C}\boldsymbol{Y}_1^{\mathrm{T}} + \boldsymbol{C}_{c2}\boldsymbol{Y}_2$$

$$\boldsymbol{A}_K = \boldsymbol{X}_1(\boldsymbol{A} + \boldsymbol{B}\boldsymbol{D}_{c11}\boldsymbol{C})\boldsymbol{Y}_1^{\mathrm{T}} + \boldsymbol{X}_2\boldsymbol{B}_{c1}\boldsymbol{C}\boldsymbol{Y}_1^{\mathrm{T}} + \boldsymbol{X}_1\boldsymbol{B}\boldsymbol{C}_{c1}\boldsymbol{Y}_2^{\mathrm{T}} + \boldsymbol{X}_2\boldsymbol{A}_c\boldsymbol{Y}_2^{\mathrm{T}} \tag{27}$$

where $\boldsymbol{X} = \begin{bmatrix} \boldsymbol{X}_1 & \boldsymbol{X}_2 \\ \boldsymbol{X}_2^{\mathrm{T}} & \boldsymbol{X}_3 \end{bmatrix}$ and $\boldsymbol{Y} = \boldsymbol{X}^{-1} = \begin{bmatrix} \boldsymbol{Y}_1 & \boldsymbol{Y}_2 \\ \boldsymbol{Y}_2^{\mathrm{T}} & \boldsymbol{Y}_3 \end{bmatrix}$.

Let $\boldsymbol{\varPi}_1 = \begin{bmatrix} \boldsymbol{X}_1 & \boldsymbol{I} \\ \boldsymbol{X}_2^{\mathrm{T}} & \boldsymbol{O} \end{bmatrix}$, $\boldsymbol{\varPi}_2 = \begin{bmatrix} \boldsymbol{I} & \boldsymbol{Y}_1 \\ \boldsymbol{O} & \boldsymbol{Y}_2^{\mathrm{T}} \end{bmatrix}$. Obviously, $\boldsymbol{\varPi}_1$ and $\boldsymbol{\varPi}_2$ are invertible, and $\boldsymbol{X} = \boldsymbol{\varPi}_1\boldsymbol{\varPi}_2^{-1}$, thus $\boldsymbol{X} > 0$ equals (25).

Pre- and postmultiply (25) by the block-diagonal matrices $\begin{bmatrix} \boldsymbol{\varPi}_2^{\mathrm{T}} & \boldsymbol{O} \\ \boldsymbol{O} & \boldsymbol{I}_{2m_c+2n_i+2m} \end{bmatrix}$ and $\begin{bmatrix} \boldsymbol{\varPi}_2 & \boldsymbol{O} \\ \boldsymbol{O} & \boldsymbol{I}_{2m_c+2n_i+2m} \end{bmatrix}$ respectively, and trim the result, thus (25) is obtained. And pre- and postmultiply (22) by the block-diagonal matrices $\begin{bmatrix} \boldsymbol{\varPi}_2^{\mathrm{T}} & \boldsymbol{O} \\ \boldsymbol{O} & \boldsymbol{I}_{2m_c+2n_i+2m} \end{bmatrix}$ and $\begin{bmatrix} \boldsymbol{\varPi}_2 & \boldsymbol{O} \\ \boldsymbol{O} & \boldsymbol{I}_{2m_c+2n_i+2m} \end{bmatrix}$, respectively, thus (23) is obtained. □

Step 4 Construct the controller.

Firstly, work out $\boldsymbol{X}_2$ by singular value decomposition. Let $\boldsymbol{U}_x\boldsymbol{S}_x\boldsymbol{V}_x^{\mathrm{T}} = \boldsymbol{X}_1 - \boldsymbol{Y}_1^{-1}$. It is obvious that $\boldsymbol{S}_x > 0$. Then, $\boldsymbol{X}_2 = \boldsymbol{U}_x\boldsymbol{S}_x^{1/2}$. Secondly, solve $\boldsymbol{B}_{c1}$, $\boldsymbol{B}_{c2}$, $\boldsymbol{C}_{c1}$, $\boldsymbol{C}_{c2}$, and $\boldsymbol{A}_c$ by $\boldsymbol{X}_1$, $\boldsymbol{X}_2$, and $\boldsymbol{A}_K$, $\boldsymbol{B}_{K1}$, $\boldsymbol{B}_{K2}$, $\boldsymbol{C}_{K1}$, $\boldsymbol{C}_{K2}$ via (27). Thirdly, solve Δ_c in real time via (26) while Δ varying. Finally, the LTI part of controller $\boldsymbol{K}$ is constructed by $\boldsymbol{A}_c$, $\boldsymbol{B}_{c1}$, $\boldsymbol{B}_{c2}$, $\boldsymbol{C}_{c1}$, $\boldsymbol{C}_{c2}$, $\boldsymbol{D}_{c11}$, $\boldsymbol{D}_{c12}$, $\boldsymbol{D}_{c21}$, $\boldsymbol{D}_{c22}$ via (2), and the varying part of controller Δ_c is exhibited via (3).

4. Autopilot design example

In this section, an air defense missile autopilot designed by the proposed algorithm is exhibited. The prescribed region is chosen as [−1 000, 0] for the real axis and [−1 000, 1 000] for the imaginary axis so as to restrain the controller fast modes. The response of the closed-loop of the missile including settling time and overshoot specifications is captured in a reference model $\boldsymbol{G}_r$. The error e_p is weighted with $\boldsymbol{W}_p$ and the $\mathcal{H}_\infty$-gain $a_{yc} \to e_p$ is minimized to force the controlled system to resemble the reference model as closely as possible. The transfer functions of $\boldsymbol{G}_a$, $\boldsymbol{G}_r$, and $\boldsymbol{W}_p$ are chosen as $\boldsymbol{G}_a(s) = \dfrac{170}{s+170}$, $\boldsymbol{G}_r(s) = \dfrac{1600}{s^2+56s+1600}$ and $\boldsymbol{W}_p(s) = \dfrac{0.5(s+840)}{s+3}$.

4.1 Static simulation

The parameter of the plant described by (2) is as follows:

$$
\boldsymbol{G}=\left[\begin{array}{cc|cccccc}
-1.432 & 1\,307.129 & -466.459 & 1.789 & 500.638 & 332.344 & -3.465 & -140.640\\
0.550 & -3.897 & 5.802 & 84.087 & 5.103 & -15.520 & -74.197 & 353.470\\
0.001 & -1.354 & -3\times10^{-4} & -3\times10^{-5} & -3\times10^{-4} & -0.111 & -0.007 & 0.120\\
-1\times10^{-4} & 0.089 & -0.004 & 5\times10^{-4} & -0.004 & -0.025 & -0.069 & 0.991\\
6\times10^{-4} & 0.005 & -2\times10^{-4} & 3\times10^{-5} & -3\times10^{-4} & 0.251 & -0.029 & -6\times10^{-4}\\
0.001 & -1.388 & 0 & 0 & 0 & 0 & 0 & 0.273\\
-3\times10^{-4} & 0.273 & 0 & 0 & 0 & 0 & 0 & 1.388\\
1 & 0 & 0 & 0 & 0 & 0 & 0 & 0\\
0 & 1 & 0 & 0 & 0 & 0 & 0 & 0
\end{array}\right].
$$

The step response of the normal acceleration a_y is illustrated in Fig. 3 and the contrastive simulation using the classical autopilot [26] is shown in Fig. 4. The classical control theory has proved itself to be a valuable and efficient tool for autopilot design, and still represents the state of the art in control system design for the applications [2,4]. Compared with Fig. 4, the specifications of the normal acceleration step response in terms of gain, overshoot and settling time of the controlled missile match those of the reference model very well independently of the parameter value in Fig. 3.

The poles map in Fig. 5 clarifies that closed-loop poles are restricted in the aforementioned region, which limits "fast modes" of the controller indirectly. On the contrary, in Fig. 6, the contrastive method [18] without limiting the fast modes will introduce "big poles" in the closed-loop system.

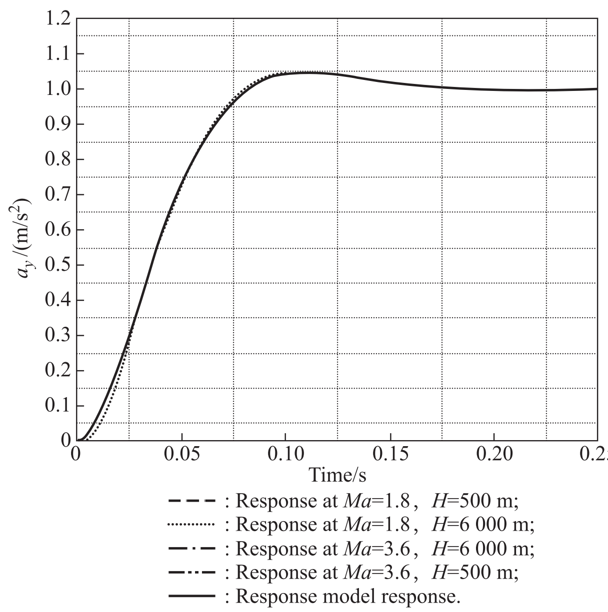

Fig. 3 Step response a_y using the proposed algorithm

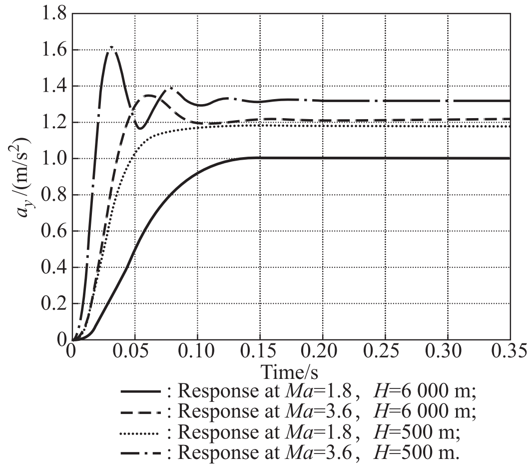

Fig. 4 Step response a_y using the classical autopilot

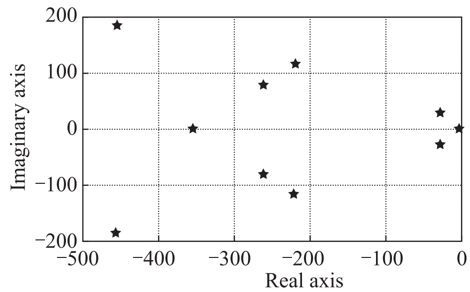

Fig. 5 Poles map using the proposed algorithm

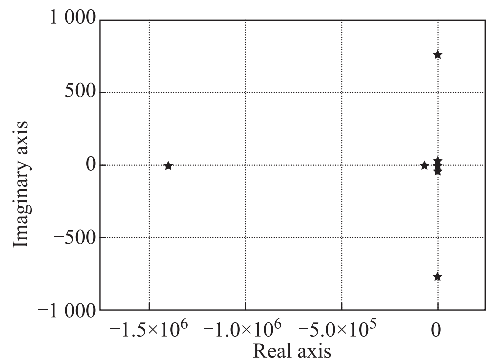

Fig. 6 Poles map using the contrastive method

4.2 Dynamic simulation

A set of nonlinear dynamic simulations are exhibited to validate the autopilot performance under parameter-varying condition. An assumption is made that the missile to be controlled is guided by certain guidance law to attack a target. The curves that flight altitude and Mach number vary with time during the controlled stage of the missile are shown in Fig. 7 respectively. In this case, the designed controller can be directly used in the simulation. The simulation results are shown in Fig. 7.

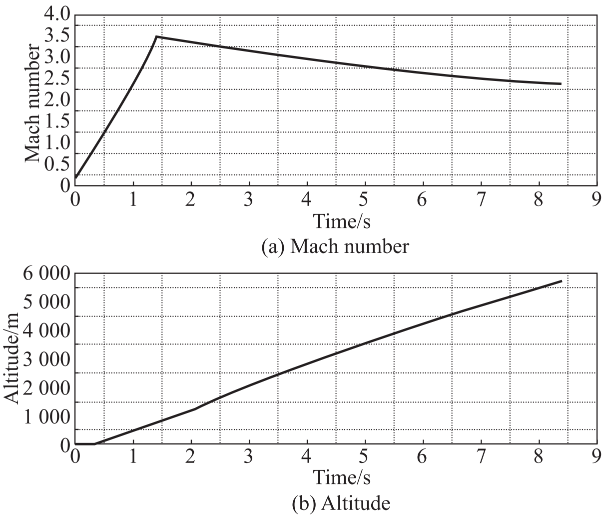

Fig. 7 Scheduling variables

Fig. 8 obviously indicates that the normal acceleration response closely follows the reference command. It also can be noticed in Fig. 8 that the settling time lasts about 0.3 s and the overshoot is lower than 10%.

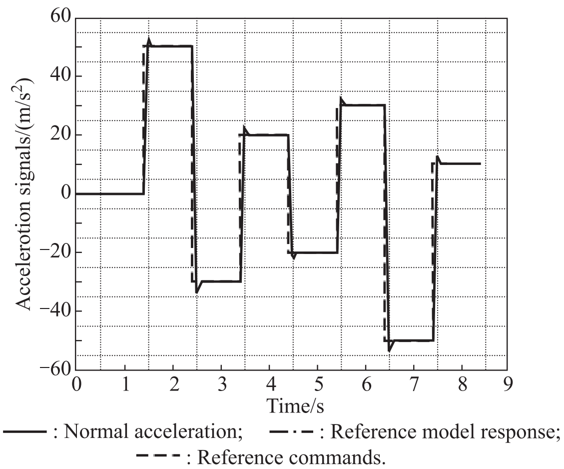

Fig. 8 Normal acceleration response curves

The pitch rate response, angle of attack response and elevator deflection response are shown in Figs. 9–11 respectively. From the response of angle of attack and elevator deflection, we can note that the trim state varies with scheduling variables. Compared with the steady state with small Mach number and low altitude, angle of attack and elevator deflection are greater than that with large Mach number and high altitude under the same command.

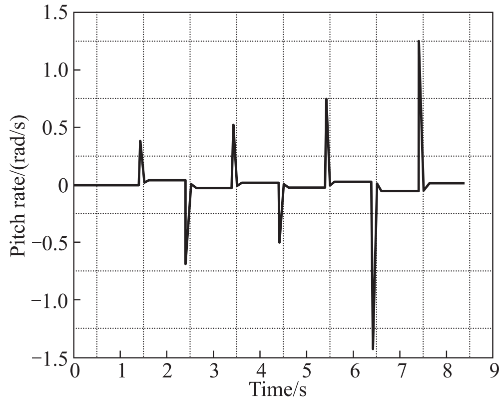

Fig. 9 Pitch rate response curve

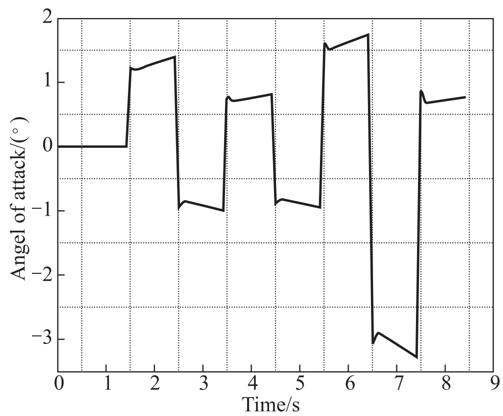

Fig. 10 Angel of attack response curve

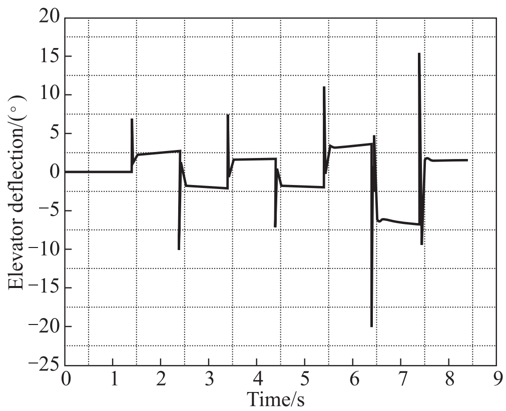

Fig. 11 Elevator deflection response curve

5. Conclusions

The efforts in this paper are directed at deriving an efficient algorithm to work out a varying controller that guarantees global and local properties, which brings in almost no conservatism. In order to achieve engineering application for high-performance flight vehicles, this algorithm is employed with certain design structure adopted in a robust LPV framework controller design. A certain air defense missile is set as the example to demonstrate the efficiency of the proposed LPV control approach with full block multiplier and regional pole placement.

The local properties, particularly the dynamic characteristics, are incarnated via the location of all the poles. A model matching structure is adopted to fulfill the designated dynamic performance specifications. The reference model involved in the autopilot design composes the generalized plant together with the missile dynamics and the actuator dynamics. And the regional pole placement scheme is involved to restrain the controller fast modes by clustering the closed-loop poles in a desired rectangle region. The global properties including robust stability and robust performance are both comprised into the notion of “robust quadratic performance”. All property specifications are generalized in the IQC frame, and then represented in proper form with full block multiplier adopted to reduce the conservatism. Finally, the representations are transformed into LMIs to design robust LPV controller in the proposed iteration so that the original problem is easily solvable through convex optimization. Static and dynamic simulations validate the performance of the designed robust LPV framework autopilot. Overall, the approach shows sufficient promise in the LPV framework autopilot design for high-performance missile.

References

[1] J. M. Biannic, P. Apkarian, W. L. Garrard. Parameter varying control of a high-performance aircraft. *Journal of Guidance, Control, and Dynamics*, 1997, 20(2): 225 – 231.

[2] G. Mattei, S. Monaco. Nonlinear autopilot design for an asymmetric missile using robust backstepping control. *Journal of Guidance, Control and Dynamics*, 2014, 37(5): 1462 – 1476.

[3] M. S. Spillman. Robust longitudinal flight control design using linear parameter-varying feedback. *Journal of Guidance, Control, and Dynamics*, 2000, 23(1): 101 – 108.

[4] C. H. Lee, B. E. Jun, J. I. Lee. Connections between linear and nonlinear missile autopilots via three-loop topology. *Journal of Guidance, Control, and Dynamics*, 2016, 39(6): 1424 – 1430.

[5] A. Packard. Gain scheduling via linear fractional transformations. *Systems & Control Letters*, 1994, 22(2): 79 – 92.

[6] P. Apkarian, P. Gahinet. A convex characterization of gain-scheduled controllers. *IEEE Trans. on Automatic Control*, 1995, 40(5): 853 – 864.

[7] F. Wu, K. Dong. Gain-scheduling control of LFT systems using parameter-dependent lyapunov functions. *Automatica*, 2006, 42(1): 39 – 50.

[8] G. H. Cai, J. M. Song, X. X. Chen. Robust LPV autopilot design for hypersonic reentry vehicle. *Aircraft Engineering and Aerospace Technology*, 2014, 86(5): 423 – 431.

[9] A. Megretski, A. Rantzer. System analysis via integral quadratic constraints. *IEEE Trans. on Automatic Control*, 1997, 42(6): 819 – 830.

[10] J. Veenman, C. W. Scherer, H. Köroglu. Robust stability and performance analysis based on integral quadratic constraints. *European Journal of Control*. http://dx.doi.org/10.1016/j.ejcon.2016.04.004i.

[11] C. W. Scherer, I. Emre Köse. Gain-scheduled control synthesis using dynamic D-scales. *IEEE Trans. on Automatic Control*, 2012, 57(9): 2219 – 2234.

[12] J. Veenman, C. W. Scherer. IQC-synthesis with general dynamic multipliers. *International Journal of Robust Nonlinear Control*, 2014, 24(17): 3027 – 3256.

[13] C. Y. Kao, M. Ravuri, A. Megretski. Control synthesis with dynamic integral quadratic constraints — LMI approach. *Proc. of the 39th IEEE Conference on Decision and Control, Australia*, 2000: 1477 – 1482.

[14] Z. Szabó, A. Marcos, D. Prieto, et al. Development of an integrated LPV/LFT framework: modeling and data-based validation tool. *IEEE Trans. on Control Systems Technology*, 2001, 19(1): 104 – 117.

[15] M. R. Breton. Gain-scheduled aircraft control using linear parameter-varying feedback. WPAFB, USA: Air Force Institute of Technology, 1996.

[16] G. M. Voorsluijs, S. Bennani, C. W. Scherer. Linear and parameter-dependent robust control techniques applied to a helicopter UAV. *Proc. of AIAA Guidance, Navigation, and Control Conference and Exhibit*, 2004: 1019 – 1030.

[17] J. Q. Yu, G. C. Luo, Z. H. Wen. Missile H_∞ gain-scheduled autopilot deign based on quasi-linear model. *Control Theory and Applications*, 2009, 26(4): 451 – 454. (in Chinese)

[18] J. Q. Yu, G. C. Luo, W. T. Yin. Missile robust gain scheduling autopilot design using full block multipliers. *Journal of Systems Engineering and Electronics*, 2010, 21(5): 883 – 891.

[19] J. Q. Yu, G. C. Luo, Y. S. Mei. Surface-to-air missile autopilot design using LQG/LTR gain scheduling method. *Chinese Journal of Aeronautics*, 2011, 24(3): 279 – 286.

[20] M. Chilali, P. Gahinet. H_∞ design with pole placement constraints: an LMI approach. *IEEE Trans. on Automatic Control*, 1996, 41(3): 358 – 367.

[21] M. Chilali, P. Gahinet, P. Apkarian. Robust pole placement in LMI regions. *IEEE Trans. on Automatic Control*, 1999, 44(12): 2257 – 2270.

[22] A. S. Ghersin, R. S. Sánchez Peña. Applied LPV control with full block multipliers and regional pole placement. *Journal of Control Science and Engineering*, 2010, 2010(3): 1 – 10.

[23] G. C. Luo, J. Q. Yu, X. Zhang. Robust regional stability: sufficient and necessary conditions. *Proc. of the Chinese Control and Decision Conference*, 2011: 1415 – 1418.

[24] C. W. Scherer. LPV control and full block multipliers. *Automatica*, 2001, 37(3): 361 – 375.

[25] I. R. Petersen. Equivalent realizations for uncertain systems with an IQC uncertainty description. *Automatica*, 2007, 43(1): 44 – 55.

[26] P. Garnell. *Guided weapon control systems*. 2nd ed. Z. K. Qi, Q. L. Xia. Beijing: Beijing Institute of Technology Press, 2003.

Biographies

Yuanchuan Shen was born in 1991. He received his B.S. degree in flight vehicle engineering from Beijing Institute of Technology, Beijing, China in 2013. Since 2013, he is a Ph.D. candidate with the School of Aerospace Engineering, Beijing Institute of Technology, Beijing, China. His research interests include flight dynamics and control, and robust control.

E-mail: shen_yuanchuan@bit.edu.cn

Jianqiao Yu was born in 1972. He received his B.S., M.S. and Ph.D. degrees from Beijing Institute of Technology in 1994, 1997 and 2007, respectively, and now he is a professor there. His main research interests include flight dynamics and control, cooperative control, flight vehicle system design and robust control.
E-mail: jianqiao@bit.edu.cn

Guanchen Luo was born in 1984. She received her B.S., M.S. and Ph.D. degrees in flight vehicle engineering from Beijing Institute of Technology, Beijing, China in 2006, 2008 and 2014, respectively. Her research interests include UAV path planning, flight dynamics and control, and robust control.
E-mail: tomato318@bit.edu.cn

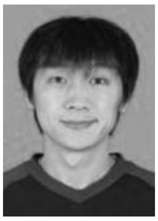

Yuesong Mei was born in 1978. He received his Ph.D. degree in flight vehicle design from Beijing Institute of Technology in 2007. He is now a lecturer at School of Aerospace Engineering, Beijing Institute of Technology. His research interests include flight vehicle system design, flight dynamics and control.
E-mail: mys001@bit.edu.cn